Lawrence Berkeley National Laboratory

Lawrence Berkeley National Laboratory

Title

Sensitivity study of CO2 storage capacity in brine aquifers with closed boundaries: Dependence on hydrogeologic properties

Permalink

https://escholarship.org/uc/item/5hb0x6tq

Authors

Zhou, Q.
Birkholzer, J.
Rutqvist, J.
et al.

Publication Date

2008-05-20

eScholarship.org Powered by the California Digital Library
University of California

CONFERENCE PROCEEDINGS

Sensitivity Study of CO_2 Storage Capacity in Brine Aquifers with Closed Boundaries: Dependence on Hydrogeologic Properties

Quanlin Zhou, Jens Birkholzer, Jonny Rutqvist, and
Chin-Fu Tsang
Earth Sciences Division, Lawrence Berkeley National Laboratory
1 Cyclotron Road, MS 90-1116, Berkeley, CA 94720

SIXTH ANNUAL CONFERENCE ON CARBON CAPTURE AND SEQUESTRATION - DOE/NETL
May 7 - 10, 2007

Abstract: In large-scale geologic storage projects, the injected volumes of CO_2 will displace huge volumes of native brine. If the designated storage formation is a closed system, e.g., a geologic unit that is compartmentalized by (almost) impermeable sealing units and/or sealing faults, the native brine cannot (easily) escape from the target reservoir. Thus the amount of supercritical CO_2 that can be stored in such a system depends ultimately on how much pore space can be made available for the added fluid owing to the compressibility of the pore structure and the fluids. To evaluate storage capacity in such closed systems, we have conducted a modeling study simulating CO_2 injection into idealized deep saline aquifers that have no (or limited) interaction with overlying, underlying, and/or adjacent units. Our focus is to evaluate the storage capacity of closed systems as a function of various reservoir parameters, hydraulic properties, compressibilities, depth, boundaries, etc. Accounting for multi-phase flow effects including dissolution of CO_2 in numerical simulations, the goal is to develop simple analytical expressions that provide estimates for storage capacity and pressure buildup in such closed systems.

1. Introduction

The CO_2 storage capacity of deep saline aquifers has usually been estimated under the assumption that the brine displacement is not a limiting factor. In other words, it is assumed that the displaced brine can easily escape from the storage reservoir and make room for the added fluid. Capacity estimates in such "open" systems are based on estimates of the total pore volume of suitable formations (i.e., those formations with sufficient injectivity and size as well as good containment of CO_2), reduced by factors that account for the limited fraction of total pore space available for CO_2 (i.e., considering heterogeneity, buoyancy effects, residual water saturation, etc.) (Bachu, 2002). A respective guidance for capacity estimates in open systems was recently developed by the Capacity and Fairways Subgroup of the Geological Working Group of the DOE Carbon Sequestration Regional Partnerships, henceforth referred to as DOE Capacity Working Group (DOE, 2006).

The purpose of this study is to investigate CO_2 injection into closed systems, where brine displacement is the limiting factor for capacity estimates. In a closed geologic system, the amount of supercritical CO_2 that can be stored in a given aquifer volume depends on how much additional pore space can be made available owing to compressibility of the pore structure and the fluids. Two aspects need to be considered: Under the assumption that CO_2 injectivity and redistribution are not a concern, the CO_2 volume that can be stored is ultimately governed by the initial pore volume, the pore compressibility, and the brine density changes in response to a maximum sustainable pressure buildup. However, in some cases the CO_2 capacity may not be limited by this theoretically available pore space, but rather by the local pressure changes near the injection zone, as the formation needs to be able to accept and redistribute the injected CO_2 with an economically reasonable injection strategy. Important parameters are then not just porosity and compressibility, but also the permeability structure of the formation (absolute value and anisotropy) and the multiphase flow properties of the CO_2-brine system. A higher permeability, for example, leads to quick migration of injected CO_2 mass away from the injection zone. In addition to these compressibility issues, dissolution of CO_2 in the brine provides another, but less important mechanism for storing CO_2.

To study the above capacity and pressure buildup issues, we have conducted TOUGH2 modeling of CO_2 injection into closed formations of different sizes assuming impermeable boundaries. Simulation results are evaluated in terms of the storage capacity for CO_2, and the simulated capacity results are compared with simple analytical expressions for storage capacity in closed-system formations. We also compare the simulated capacities for closed systems with capacity estimates for open systems provided by the DOE Capacity Working Group (DOE, 2006). Sensitivity studies are conducted for varying different aquifer properties.

How realistic is the assumption of closed systems for CO_2 target formations? It is probably fair to say that most saline systems designated for CO_2 sequestration would not be "closed"; i.e., there would be more or less permeable boundaries that allow the displaced brine to escape. On the other hand, zones of abnormal pressure, much higher than hydrostatic, have been observed in many sedimentary basins around the world (e.g., Neuzil, 1995; Muggerigdge et al., 2004). These are typically "closed" volumes of higher-permeability rock surrounded on all sides by low-permeability barriers, where abnormal pressures have been maintained over geologic times. There is a conundrum when using these closed systems for carbon sequestration. Closed systems would be ideal for CO_2 containment, because the low-permeability barriers would prohibit leakage from the target formation, but since

the displaced brine cannot escape either, the capacity for CO_2 storage may be rather small. To evaluate under which conditions target formations are to be considered closed or open with respect to brine displacement, we have evaluated additional sensitivity cases with caprock and baserock units that have small, but not zero permeability. We demonstrate that very small seal permeabilities (e.g., $< 10^{-20}$ m^2 for the considered cases) indeed exhibit closed-system behavior, as only a small fraction of brine escapes through the caprock or baserock. However, slightly larger seal permeabilities (e.g., order of 10^{-17} m^2 for the considered case) may create an "open" system with respect to brine leakage, while still allowing for sufficient trapping of injected CO_2.

2. TOUGH2 Simulations and Results

A TOUGH2 model was developed simulating the two-phase flow in a deep saline aquifer during CO_2 injection over 30 years. The target formation is located at a depth of approximately 1,200 m (top of formation) below the ground surface (see Figure 1). The radial, two-dimensional model domain used for the modeling is 250 m thick and has different extents in the radial direction. The cases modeled have radial extents of 100, 50, 30, 20, and 10 km. The domain is bounded at the top and bottom by sealing layers, which are assumed to be impervious in the base cases. The outside vertical boundary is a no-flow boundary (closed system). An injection zone is introduced at the center, with a total injection rate of 120 kg/s uniformly distributed along its screen over 125 m in the lower half of the aquifer. This corresponds to a large carbon source with an annual output of about 3.8 million tones of CO_2. The CO_2 injection continues over 30 years. The injection zone covers an area of radius 50 m, representing not a single well, but rather a few distributed wells, to improve injectivity and reduce local pressure buildup. For each simulation run, the aquifer is initially fully water-saturated, assuming a hydrostatic fluid pressure distribution in the vertical direction. The ECO2N module of the TOUGH2 code (Pruess, 2005) is used to simulate the transient CO_2-water flow over the 30-year injection period.

Typical values of hydrogeologic properties were used to represent a homogeneous brine aquifer (see Table 1). The pore compressibility is 4.5×10^{-10} Pa^{-1}, a value representative of structurally sound sandstone (Harris, 2006). The permeability of the storage formation is 10^{-13} m^2. Pore compressibility is one of the key aquifer properties of a closed-system aquifer for providing increased pore space (or porosity) to store the injected CO_2, while permeability is one of the key aquifer properties for the movement and spatial distribution of CO_2. Note that the compressibility of brine is automatically taken into account in TOUGH2 in terms of density variation with fluid pressure. Unlike many groundwater flow simulators, which employ specific storativity to describe the combined effect of matrix and fluid compressibility, TOUGH2 separates the effect of porosity changes and density variation. Brine compressibility is mildly affected by total pressure and temperature in the P-T range relevant for CO_2 storage. For the conditions at the top of the aquifer depicted in Figure 1, with a pressure of 120 bar and a temperature of 40 ^{o}C, brine compressibility is on the order of 3.9×10^{-10} Pa^{-1}.

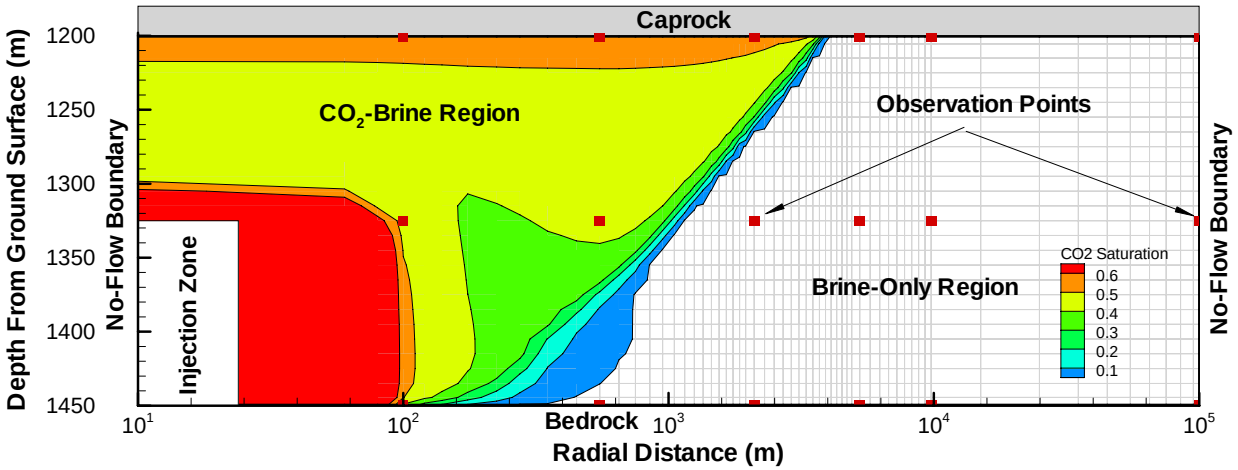

Figure 1. Schematic of the "closed" deep brine aquifer for CO_2 injection, with numerical mesh and observation points for the transient features of the aquifer in response to the CO_2 injection. The figure shows a large target formation with a radial extent of 100 km.

Table 1. Typical values of saline-aquifer hydrogeologic properties used in the simulations

Properties	**Values**
Permeability (m^2)	1.0E-13
Pore Compressibility (Pa^{-1})	4.5E-10
Porosity	0.12
Van Genuchten m	0.46
Van Genuchten alpha (Pa^{-1})	5.1E-5
Residual CO_2 saturation	0.05
Residual water saturation	0.30

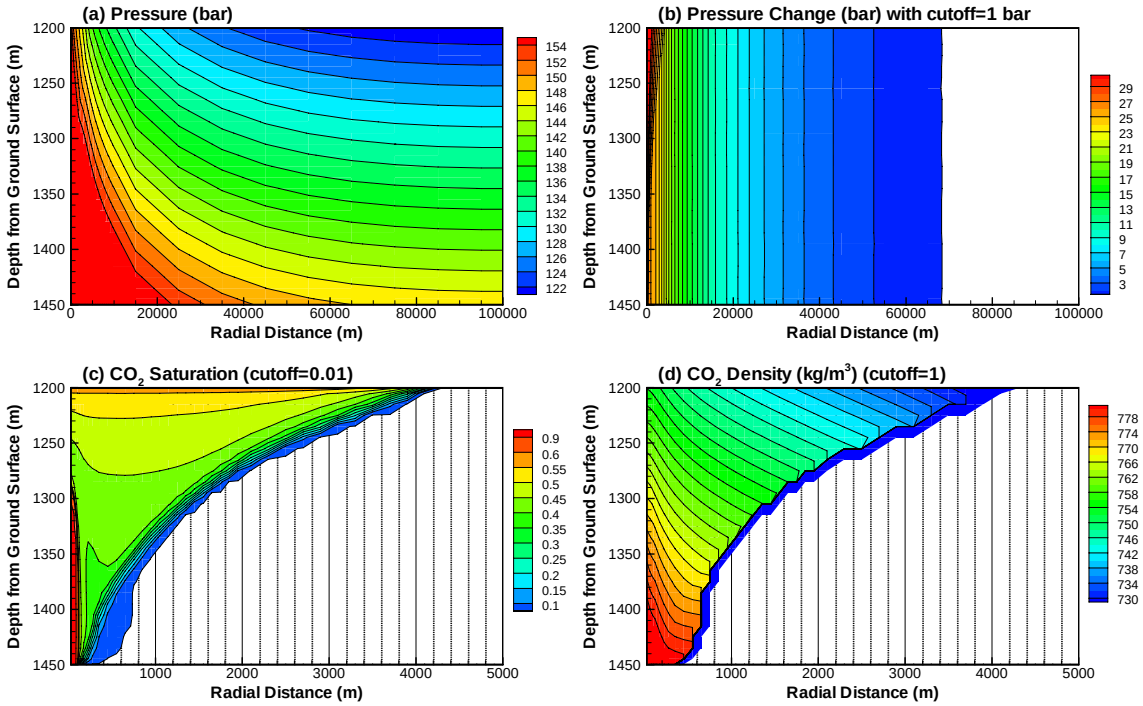

Figure 2. Spatial distribution of (a) fluid pressure, (b) pressure buildup or change in fluid pressure from the initial hydrostatic condition, (c) CO_2 saturation, and (d) CO_2 density, at the end of CO_2 injection (30 years) simulated for the "closed" domain with a 100 km radial extent. Figures (c) and (d) show close-ups of the CO_2 plume (region with two-phase system of CO_2 and brine).

Figures 2 and 3 show spatial distributions of pressure, pressure buildup, CO_2 saturation, and CO_2 density at the end of the injection period (30 years) for the cases with a model domain extending 100 km and 20 km, respectively. As evident from Figures 2a and 2b, the larger domain stores the injected CO_2 without considerable pressure increase at the lateral boundary (less than 1 bar). In other words, the pressure buildup represents that of an open system, where the lateral boundary is not felt. The local buildup in the vicinity of the injection zone (about 32 bar) is a result of CO_2 pushing brine outward. For the smaller system of 20 km radial extent, the pressure buildup varies from 68 bars within the injection zone to 45 bars at the outer radial boundary. Since the displaced brine can not escape, the entire formation becomes an overpressured system, with the storage capacity provided by pore and fluid compressibility in response to the pressure buildup. There is some local pressure buildup close to the injection zone, creating a driving force for the displacement of brine, but this time the local pressure buildup is in addition to a formation-scale pressure buildup, caused by the necessity to provide sufficient storage capacity.

One may argue whether the observed pressure buildup in the 20-km case is tolerable. Obviously, geomechanical degradation to the sealing structures (such as microfracturing and/or fault reactivation) needs to be avoided. We may assume here a maximum tolerable pressure buildup of 60 bar—corresponding to 50% of the initial hydrostatic pressure at the top of the formation—which means that the total fluid pressure is much less than the

lithostatic value. With a maximum tolerable pressure increase of 60 bar, the 20 km case is close to or at its capacity limits after 30 years of injection. Note that for real target formations, the maximum tolerable pressure increase should be reviewed in a case-by-case assessment, taking into account initial stress fields and geomechanical properties of the rock units at the selected sites.

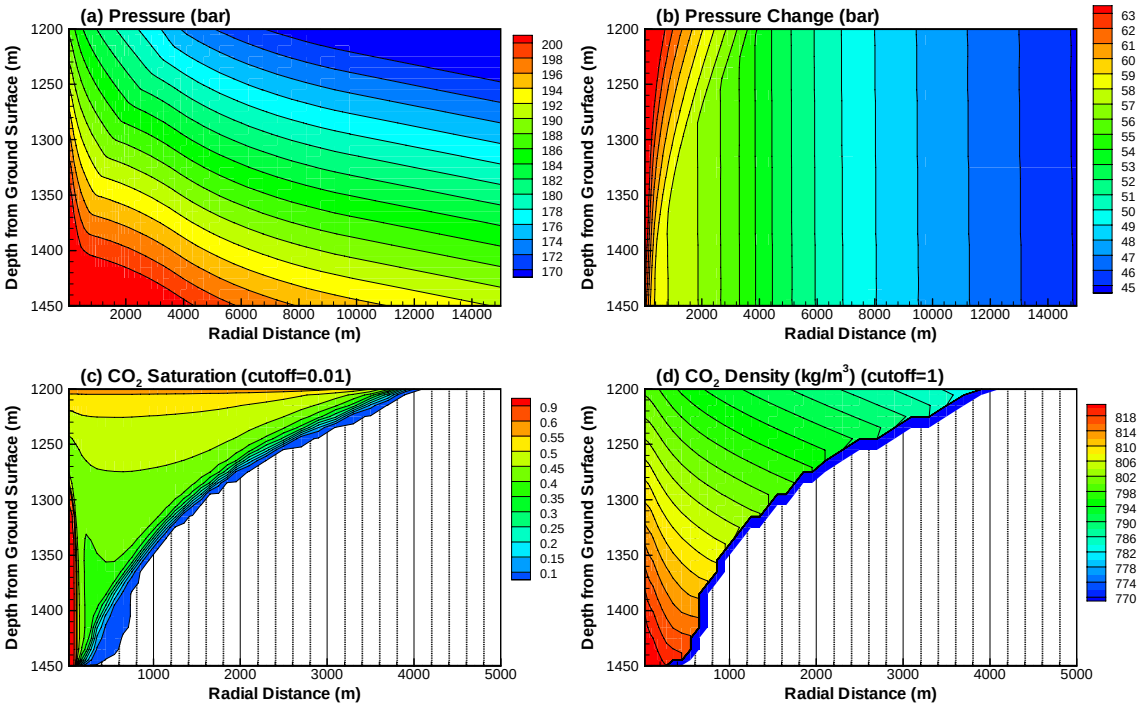

Figure 3. Spatial distribution of (a) fluid pressure, (b) pressure buildup or change in fluid pressure from the initial hydrostatic condition, (c) CO_2 saturation, and (d) CO_2 density, at the end of CO_2 injection (30 years) simulated for the "closed" domain with a 20 km radial extent. Figures (c) and (d) show close-ups of the CO_2 plume (region with two-phase system of CO_2 and brine).

Comparison of Figures 2 and 3 indicates that the CO_2 plumes in both cases, with 100 km and 20 km radial extent, are generally similar in shape, despite different pressure conditions. Minor differences can be seen in the lateral extent of the plumes. The plume size is slightly smaller for the 20 km case, because the increased pressure translates into a higher CO_2 density (see Figures 2d and 3d). Remember that the total CO_2 mass injected into the formation is the same at the end of the 30-year injection period for both cases.

Figure 4 shows pressure buildup as a function of radius for all simulation cases, with radial extent varying from 100 km to 10 km, and at different times after injection start. Notice the different scales of the horizontal and vertical axes. In all cases, the early pressure buildup from injection propagates away from the injection zone, with the propagation velocity dependent on pore and brine compressibility values, porosity, and permeability. Except for the case with 100 km radial extent, the pressure buildup eventually reaches the outer boundary. The smaller the formation, the sooner this happens, and the higher the overall pressure buildup at the end of injection period. In the 10 km case, the total pressure actually reaches an unrealistically high level, with maximum values above 300 bar. Injection would need to cease after about 12 years, because the maximum tolerable pressure buildup of 60 bar would then be exceeded.

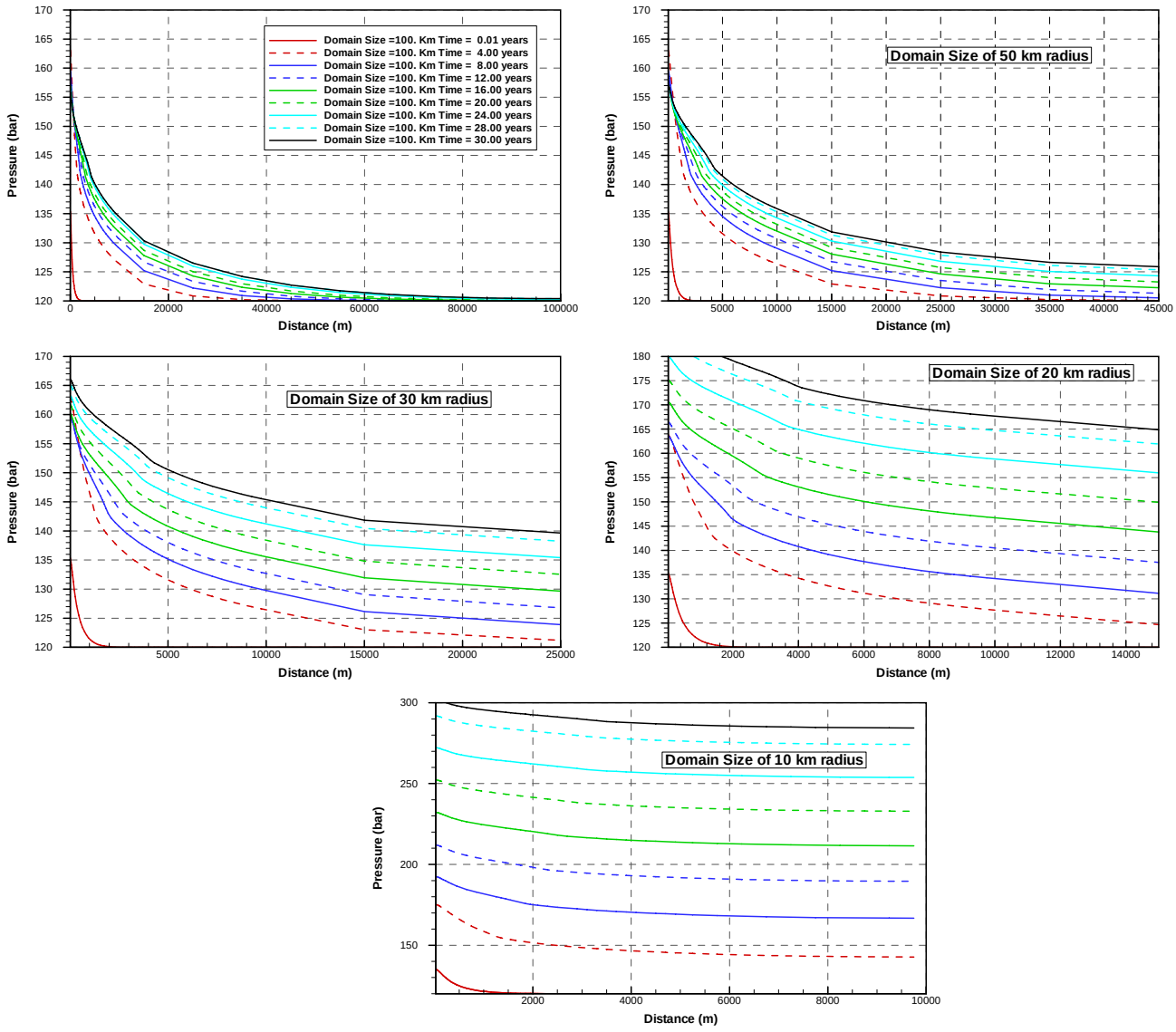

Figure 4. Fluid-pressure profiles for different domain sizes and different times after injection start

Figure 5 shows the pressure-buildup profiles of all cases at selected times in one plot, for easy comparison between different domain sizes. The profiles show that the pressure evolution is identical for the different domain sizes as long as the pressure pulse has not reached the boundary. Once the pressure pulse reaches the boundary, the pressure values increase beyond those of the other cases with larger radial extent. Again, the smaller the domain, the sooner this happens. For example, at 2 years after injection start, only the smallest domain, with 10 km radial extent, deviates from the other cases because the pressure pulse has arrived at the outer boundary. The 20 km domain has started to deviate at 4 years, the 30 km domain has started to deviate at 20 years, and the 50 km domain shows a minor deviation from the 100 km domain at 30 years.

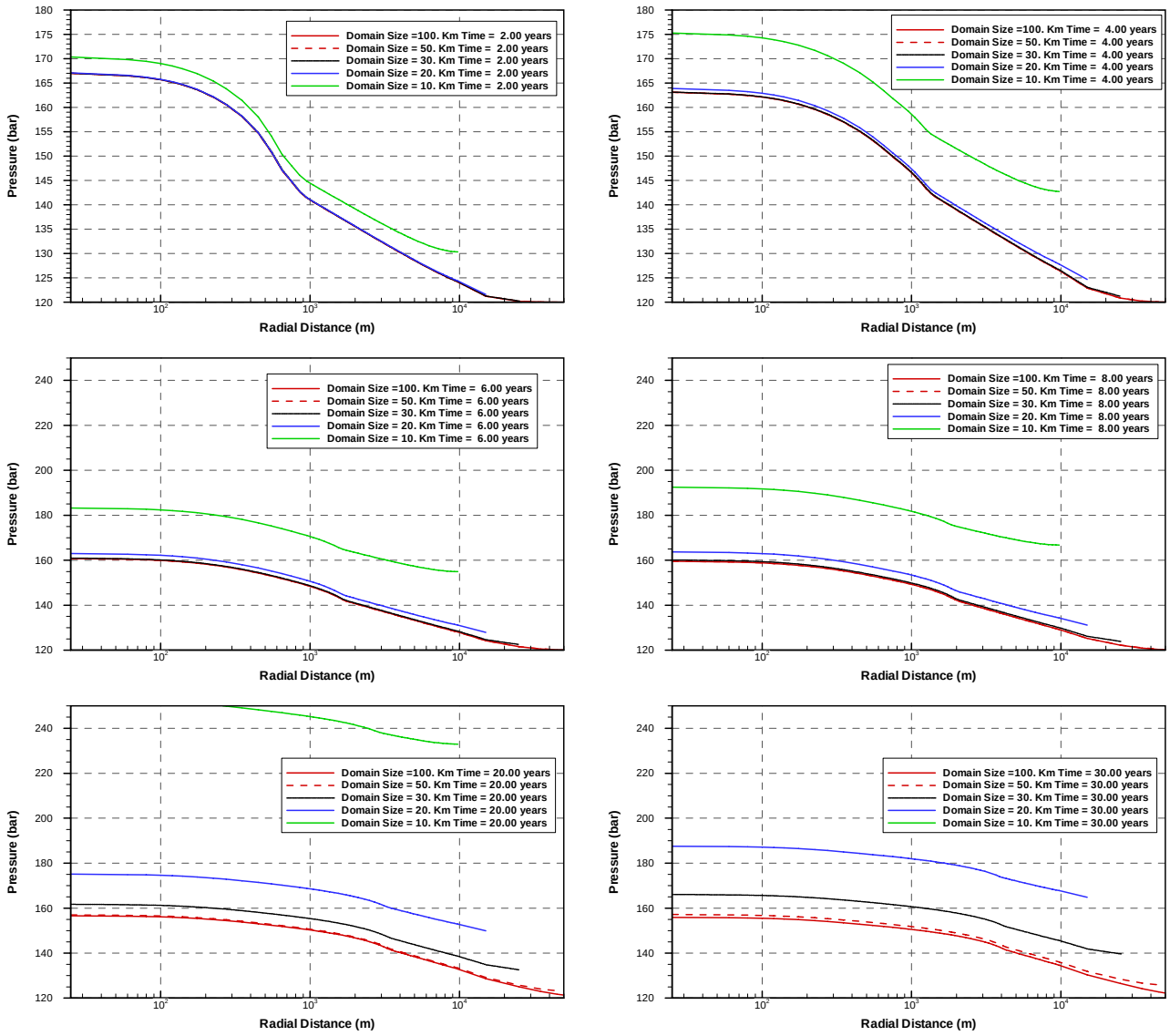

Figure 5. Fluid pressure profiles for different times after injection start and different domain sizes (radial distance shown in log scale)

3. Comparison with Simple Capacity Estimates

We use these simulation results from the previous section to derive estimates of storage capacity in closed systems. We compare the simulated capacities with those obtained from simple analytical estimates for closed systems, as well as those previously suggested for open systems (DOE, 2006).

Estimates for Open Brine Systems

A methodology for estimating the storage capacity of open systems was proposed by the DOE Capacity Working Group (DOE, 2006). A simple formula was given as follows (see explanation of parameters in Table 2):

$$G_{CO2} = \rho\, V_{CO2} = \rho\, A\, h_g\, \phi_{tot}\, E \qquad (1)$$

Table 2. Parameters and units used in Equation (1)

Parameter	Units*	Description
G_{CO2}	M	Mass estimate of brine-formation CO_2 storage capacity
ρ	M/L^3	Density of CO_2 evaluated at pressure and temperature that represents storage conditions anticipated for a specific geologic unit averaged over h_g
V_{CO2}	L^3	Volume estimate of brine-formation CO_2 storage capacity at storage conditions
A	L^2	Geographical area that defines the basin or region being assessed for CO_2 storage-capacity calculation
h_g	L	Gross thickness of brine formations for which CO_2 storage is assessed within the basin or region defined by A
ϕ_{tot}	L^3/L^3	Average porosity of brine formation for which CO_2 storage is assessed within the basin or region defined by A
E	L^3/L^3	CO_2 storage efficiency factor that reflects the fraction of the total pore volume filled by CO_2

* L is length; M is mass

In the above formula, the efficiency factor E reflects the fraction of the total available pore volume in a given basin/region that CO_2 can be stored in. There are two basic sets of contributions to E. "Basin-scale" contributions account for the fact that only a subset of the considered basin/region has suitable formations for geologic sequestration, in terms of minimum permeability and porosity for containment and formation interconnectivity. "Formation-scale" contributions reduce the net pore volume available for CO_2 storage in a suitable formation, owing to areal displacement efficiency, vertical displacement efficiency, gravity effects, and microscopic displacement. These formation-scale contributions are listed in Table 3 (DOE, 2006), where the numbers in parentheses give the estimated range of values for each efficiency factor. The maximum and minimum are meant to be reasonable high and low values. The final efficiency is the multiplicative combination of the above individual contributions and can be obtained, for example, through Monte Carlo simulations (DOE, 2006).

To exemplify the resulting efficiency of open systems, let us assume we have identified a suitable formation for CO_2 sequestration. This means that we do not need to apply the basin-scale efficiency for CO_2 storage calculation, but we do need to apply formation-scale contributions. We can use the above given reduction factors E_A, E_I, E_g, and E_d to estimate the fraction of the effective pore volume available for storage, and then calculate the total volume V_{CO2} or the total mass G_{CO2} from Equation (1) above, provided that we know area A, thickness h_g, effective porosity ϕ_{eff}, and density ρ of CO_2 at the storage conditions. Using average values for the reduction factors, we end up at $0.65 \times 0.75 \times 0.4 \times 0.65 \approx 0.13$. Using minimum values gives $0.5 \times 0.6 \times 0.2 \times 0.5 \approx 0.03$; using maximum values gives $0.8 \times 0.9 \times 0.6 \times 0.8 \approx 0.35$. The resulting efficiency range, with a most likely value of 0.13, a minimum of 0.03 and a maximum of 0.35, represents the estimated portion of the formation's porosity available for CO_2 storage in an open system; i.e., in a system where the displaced brine can easily escape without further consideration. For comparison with the simulated closed systems, we have used the most likely efficiency value to estimate the total storage capacity of open formations with 250 m thickness and 100, 50, 30, 20, and 10 km in radial extent (see Table 4).

Table 3. Formation-Scale Efficiency Factors from DOE (2006)

Areal displacement efficiency	E_A (0.5–0.8)	Fraction of immediate area surrounding an injection well that can be contacted by CO_2
Vertical displacement efficiency	E_I (0.6–0.9)	Fraction of vertical cross section (thickness), with the volume defined by the area that can be contacted by the CO_2 plume from a single well; most likely influenced by variations in porosity and permeability between sublayers in the same geologic unit.
Gravity	E_g (0.2–0.6)	Fraction of net thickness that is contacted by CO_2 as a consequence of the density difference between CO_2 and *in situ* water. In other words, 1-E_g is that portion of the net thickness not contacted by CO_2 because the CO_2 rises within the geologic unit.
Microscopic displacement efficiency	E_d (0.5–0.8)	Portion of the CO_2-contacted, water-filled pore volume that can be replaced by CO_2. E_d is directly related to irreducible water saturation in the presence of CO_2

Estimates for Closed Brine Systems

A similar methodology for estimating capacity can be applied for closed systems. We can use the same basic formula given in Equation (1), but now define the efficiency factor based on the pore compressibility and the brine density changes in response to a maximum tolerable fluid pressure buildup. Since it is assumed that brine cannot escape from the formation, the available volume for storage of CO_2 is provided by the expansion of the pore volume plus the increased density of the water body. To simplify, we assume that the entire formation experiences a uniform pressure buildup up to a maximum value defined as the maximum tolerable pressure buildup. We refer to this simple estimate as the theoretically available storage capacity in a closed system. Using a maximum tolerable pressure buildup of 60 bar and a pore compressibility of 4.5×10^{-10} Pa^{-1} (similar to the simulation examples), the pore volume in a closed system would expand by 0.0027 times the initial pore volume. Thus, the efficiency contribution from pore volume expansion, E_P, is 0.0027. The density change of brine from 1105.47 kg/m^3 at 120 bar to 1107.96 kg/m^3 at 180 bar would provide another 0.0023 times the initial pore volume. Thus, the efficiency contribution from brine density changes, E_B, is 0.0023. Together, the estimated total efficiency in a closed system would be 0.005, much lower than in an open system. See Table 4 for the estimated total storage capacity of a closed formation with 250 m thickness and 100, 50, 30, 20, and 10 km in radial extent. Analogous to Equation (1), a simple formula for closed-system storage capacity would be given as follows:

$$G_{CO2}\ (\text{closed}) = \rho\ V_{CO2}\ (\text{closed}) = \rho\ A\ h_g\ \phi_{tot}\ (E_P + E_B) \qquad (2)$$

The estimated efficiency in a closed system is sensitive to the pore compressibility of the selected formation. It is also affected by the maximum tolerable pressure buildup that the formation and the sealing units are expected to sustain. (It is less affected by sensitivities to brine compressibility, which is fairly constant over the range of pressure and temperature conditions relevant for CO_2 storage.) Wide ranges of pore (or matrix) compressibility can be found in the literature, reflecting different types of subsurface material (e.g., Fjar et al., 1991; Domenico and Schwartz, 1998; Hart, 2000; Harris, 2006). In the simulation runs above, a pore compressibility value of 4.5×10^{-10} Pa^{-1} was used, representative of sound sandstone in deep formations (Harris, 2006). Domenico and Schwartz (1998) give ranges of compressibility values for different materials, such as less than 3.3×10^{-10} Pa^{-1} for sound rock, 3.3×10^{-10} Pa^{-1} through 6.9×10^{-10} Pa^{-1} for fractured rock, or 1×10^{-8} Pa^{-1} through 5.2×10^{-9} Pa^{-1} for dense sandy gravel. Even higher compressibilities can be expected in plastic or unconsolidated materials (e.g., on the order of 10^{-6} or 10^{-7} Pa^{-1} for plastic clay), which are, of course, not typically relevant for deep geological storage of CO_2. On the other end of the spectrum, the lowest range measured from laboratory tests by Hart (2000) is 7.0×10^{-11} Pa^{-1}. This wide range may have a significant impact on the CO_2 storage capacity in closed systems. Assuming reasonable pore compressibilities for deep formations ranging from 4.5×10^{-9} Pa^{-1} to 4.5×10^{-11} Pa^{-1}, the estimated efficiency contribution from pore expansion (at a maximum pressure buildup of 60 bar) would range from 0.027 to 0.00027. Adding the brine compressibility contribution would give total efficiency ranging from 0.029 to 0.0025. The upper value is close to the estimated minimum efficiency of an open system.

Table 4 gives a summary of capacity estimates for open and closed systems with domain sizes and properties equal to the simulation study in Section 4.2. For open systems, we use Equation (1) with an average efficiency of

0.13. For closed systems, we use Equation (2) with a total efficiency of 0.005, based on a pore compressibility of 4.5×10^{-10} Pa^{-1} and a maximum tolerable pressure buildup of 60 bar. These capacity estimates are compared with the actual capacities calculated from the simulation results, after injection of a total mass of about 114 million tonnes of CO_2 after 30 years of injection. Capacities are given in CO_2 volume here; they need to be converted to mass, if necessary, using the CO_2 density at the given P-T conditions. The simulated CO_2 volumes represent CO_2 residing in its own phase, not the smaller amount that is dissolved in water. The estimated capacity values clearly demonstrate the fundamentally different storage capacities in open and closed systems, with the former offering much higher storage potential. Comparison of simulated storage volumes and estimated capacities of closed systems shows that the simple estimates using a maximum tolerable pressure buildup work quite well. All domain sizes larger than a 20 km radial extent have an average pressure buildup less than the tolerable value and have total CO_2 volume less than the estimated capacity. That is, they are not yet at their capacity limit, with the 100 km case much below the limit and the 20 km case close at the limit. The 10-km case, on the other hand, has unreasonably high fluid pressure after injection of CO_2. Here, the stored volume of CO_2 greatly exceeds the estimated maximum capacity. A simple a-priori estimate of the maximum capacity using Equation (2) would have indicated that a closed system of 10 km radial extent and the given properties would not be able to store the desired amount of CO_2.

Table 4. Comparison of CO_2 storage volume in a closed system using numerical simulation results compared to capacity estimates for a closed system and open systems, after 30 years of injection

		Simulated Results			Estimated	Estimated
Domain Radius (km)	Initial Pore Volume (10^9 m^3)	Total Stored CO_2 Volume* (10^9 m^3)	Average Pressure Buildup (bar)	Ratio CO_2 Volume to Initial Pore Volume (-)	Closed System Capacity with E = 0.005 (10^9 m^3)	Open System Capacity with E = 0.13 (10^9 m^3)
100	942.5	0.139	2.0	0.00015	4.713	122.5
50	235.6	0.138	7.9	0.00059	1.178	30.6
30	84.8	0.136	21.4	0.0016	0.424	11.0
20	37.7	0.131	46.4	0.0035	0.189	4.9
10	9.4	0.117	166.0	0.0124	0.047	1.2

* Injected mass is identical for all domains. Stored volumes differ slightly because of different pressure/density conditions.

4. Impact of Additional Storage Mechanisms in Closed Brine Systems

The simplified storage calculations for closed systems (Equation (2)) neglect details of CO_2 flow and storage mechanisms which, if included, would affect the estimates in both directions. For example, dissolution of CO_2 into the water phase would allow for more carbon storage in a closed system. Also, closed systems are never really “closed”; i.e., even if the formation was confined by caprock and baserock units, and was laterally constrained by sealing faults, the low-permeability seals would allow for some amount of brine to leave the system. An opposite effect would be the local pressure buildup near the injection zone. Depending on the injectivity of the formation and the selected injection pattern, the maximum sustainable pressure in a closed system may be reached locally, but may not uniformly extend over the entire area. This, in turn, would reduce the storage capacity of a closed formation. Below, we describe some additional studies aiming to evaluate the importance of these additional factors and their related sensitivities.

The effectiveness of dissolution of CO_2 into the water phase depends on various factors: including the solubility of CO_2 in water (around 0.01 to 0.03 in mass fraction) and the degree of contact between the CO_2 and the water phase. For example, a disperse CO_2 plume in a heterogeneous system in a flowing groundwater body will dissolve more CO_2 than a rather compact stagnant plume. In our simulation examples, the total dissolved fraction of CO_2, relative to the total injected CO_2 mass, is on the order of 7% at the end of injection. Without going into detail, we may assume that a value of 10% dissolved CO_2 mass is a reasonable bounding value for the short-term (i.e., injection-phase) efficiency of dissolution. Given the nature of the closed-system estimates, it is probably not necessary to explicitly account for dissolution in the simple capacity calculations.

In the simulation runs discussed in Section 2, the caprock was assumed to be impervious. However, the literature shows that caprock or shale has a wide range of permeability from 10^{-23} to 10^{-16} m^2 (Neuzil, 1994; Domenico and Schwartz, 1998; Hart et al., 2006). To check on the importance of water losses through low-permeability cap- and baserocks, we conducted additional simulations for the domain with a 20 km radial extent. Instead of having impermeable seals, we modeled over- and underlying units with 60 m thickness each and permeability values of 10^{-20}, 10^{-19}, and 10^{-18}, 10^{-17} m^2. The porosity in these units is 0.05, and the van Genuchten alpha value is 5.1×10^{-6} Pa^{-1} (representing roughly the inverse of entry pressure for the nonwetting phase); all other properties are identical to those for the storage formation. It is assumed that any overpressure developing within the storage formation diminishes within the cap- and baserock units. In the model, fixed pressure conditions equal to hydrostatic are set at the top of the upper seal and the bottom of the lower seal. Figure 6 and Table 5 give results from the sensitivity simulations.

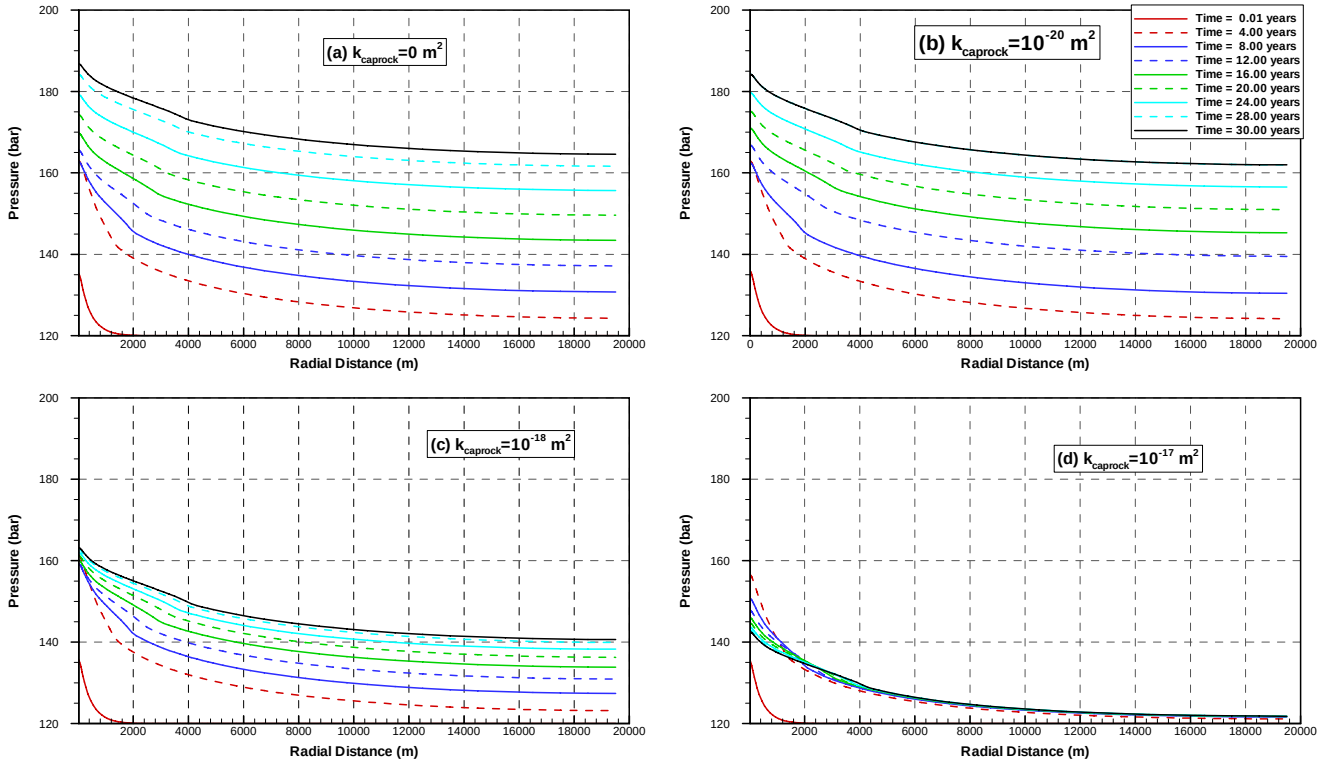

Figure 6. Fluid pressure profiles at different times for four cases of caprock permeability. The domain size is 20 km in radial extent.

The pressure profiles in Figure 6 suggest that a seal permeability of 10^{-20} m^2 gives results similar to those obtained in the case with impermeable seal. Further increases in permeability have a stronger impact, evident from the pressure buildup in the storage formation being considerably less than in the other cases. Some fraction of the displaced brine escapes from the storage formation through the seals, and provides enough additional storage capacity for the injected CO_2 such that less pressure buildup occurs. Table 5 gives the ratio of leaked brine volume to total CO_2 volume stored in phase. With a seal permeability of 10^{-20} m^2, this ratio is rather small at 0.061. With a seal permeability of 10^{-17} m^2, on the other hand, this fraction increases to 0.92. In this case, the additional CO_2 storage capacity from brine leakage would amount to about 92% of the totally injected CO_2 after 30 years. Thus, this effect can be important for storage-capacity estimates in realistic "closed" systems that have sealing units with small, but not zero permeability. For simple geometries, given seal permeability, and given pressure buildup, the brine leakage through seals can be determined a priori from analytical Darcy flow calculations in the seal units, and its importance on storage capacity estimates can be evaluated. Notice that for non-zero seal permeabilities, a small amount of CO_2 escapes from the formation into the caprock (Table 5). This amount is much smaller than the brine leakage. CO_2 as the nonwetting fluid needs to overcome a considerable entry pressure before being able to migrate into the brine-filled seal pores.

Table 5. Comparison between injected CO_2 mass and volume and brine mass and volume leaked through top and bottom seals as function of permeability, after 30 years of injection (formation permeability is 10^{-13} m^2.

Seal Permeability (m^2)	Injected CO_2	Leaked Brine*		Leaked CO_2*
	Total Stored CO_2 Volume (10^6 m^3)	Total Leaked Brine Volume (10^6 m^3)	Ratio Leaked Brine Volume to CO_2 Stored Volume (-)	Ratio Leaked CO_2 Volume to CO_2 Stored Volume (-)
0	131	0	0.0	0
10^{-20}	134	8.2	0.061	0.0014
10^{-19}	135	24.6	0.182	0.0028
10^{-18}	139	76.7	0.555	0.0064
10^{-17}	151	139.2	0.922	0.0301

* Leaked volumes are given for flow through interface between storage formation and cap- or baserock.

A final set of simulations cases explores sensitivity with respect to the local pressure buildup near the injection zone. Again choosing the 20 km domain as an example, we modeled three additional cases, varying the formation permeability from the base-case value of 10^{-13} m^2 to values of 10^{-12} m^2, 5×10^{-13} m^2, and 5×10^{-14} m^2. For larger permeabilities, the pressure buildup in the formation extends more uniformly over the entire area (see Figure 7). This would increase the storage capacity of a closed formation, because local pressure buildup due to injection is limited. The opposite effect is seen with the smaller permeability value, where a strong local pressure buildup near the injection zone leads to total fluid pressure in excess of the desired maximum pressure (around 180 bar). Thus, issues of local pressure buildup may need to be considered when estimating the storage capacity in closed systems with rather small permeability.

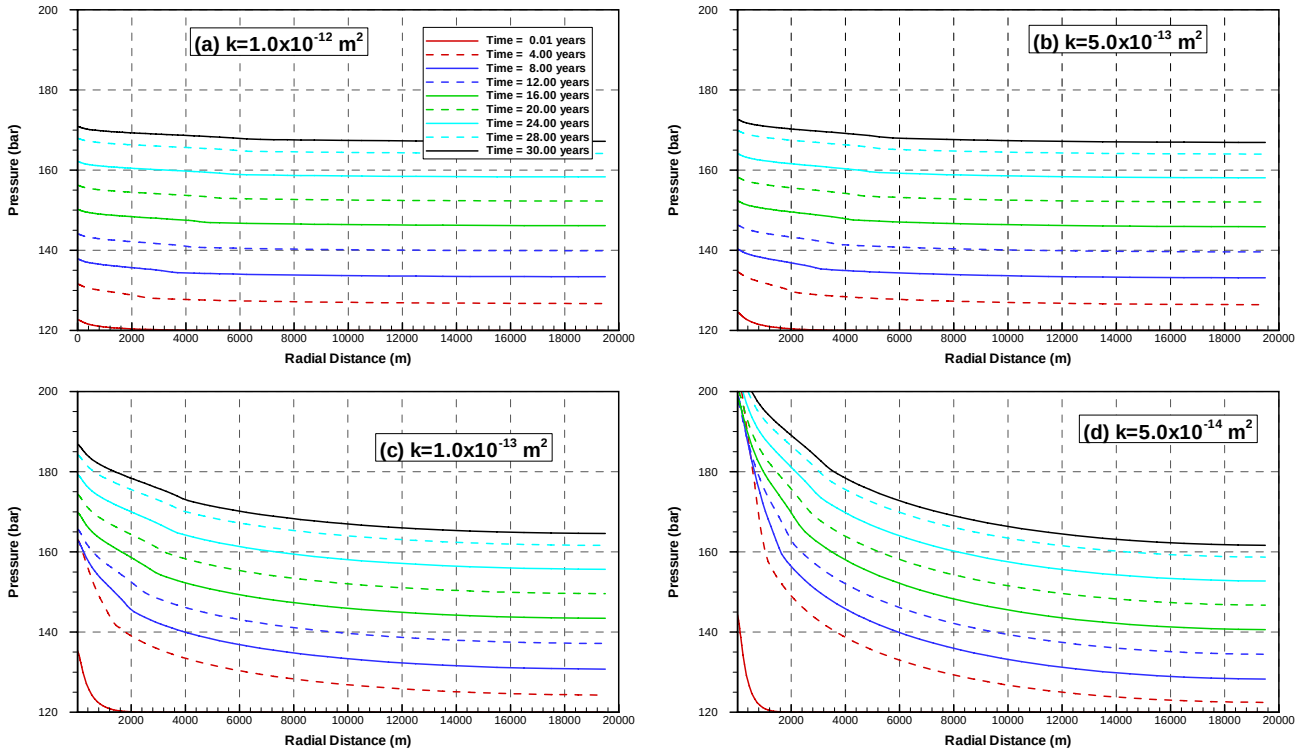

Figure 7. Fluid pressure profiles at different times for four cases of storage formation permeability. The domain size is 20 km in radial extent.

5. Summary and Conclusions

- The available volume for CO_2 storage in closed systems is mostly provided by pore compressibility and brine compressibility in response to formation pressure buildup.
- Simplified capacity estimates can be derived using Equation (2), where the total available pore space in a suitable formation is adjusted with efficiency factors that account for pore and brine compressibility. The capacity estimates are based on a maximum tolerable pressure buildup in the formation, to be selected based on geomechanical assessments.
- A typical formation-scale efficiency factor of 0.005 was estimated for the conditions studied in this paper, with similar contributions from both pore and brine compressibility. However, pore compressibility can vary widely depending on the formation materials. For reasonable pore compressibility values between 4.5×10^{-9} Pa^{-1} to 4.5×10^{-11} Pa^{-1}, the estimated total efficiency factor would range from 0.029 to 0.0025. Compared to this, DOE (2006) suggests formation-scale efficiency factors in open systems between 0.03 and 0.35, with a best estimate of 0.13.
- Additional factors important for storage capacity in closed systems have been evaluated that are neglected in the simplified capacity estimates from Equation (2). These are the impact of dissolution (moderately important) and the impact of localized pressure buildup near injection zones (important for formation permeabilities below a certain threshold; implications on optimal injection strategy).
- Brine leakage through confining units that are not impermeable becomes important for seal permeabilities above a certain threshold, in this study estimated around 10^{-18} m^2. Seal permeabilities above the threshold may create an "open" system with respect to displacement of brine, while still allowing for sufficient trapping of injected CO_2. Seal permeabilities below 10^{-19} m^2 exhibit closed-system behavior, as only a small fraction of brine escapes through the caprock or baserock.

References

Bachu, S., 2002. Sequestration of CO2 in geological media in response to climate change: road map for site selection using the transform of the geological space into the CO2 phase space, *Energy Conversion & Management*, 43, 87–102.

DOE, 2006. Proposed Methodology for Construction of a 2006 National Geological Carbon Sequestration Capacity Assessment, Final Draft. Prepared by the Capacity and Fairways Subgroup of the Geologic Working Group of the DOE Carbon Sequestration Regional Partnerships, October 1, 2006.

Domenico P.A., and F.W. Schwartz, 1998. *Physical and Chemical Hydrogeology, 2nd edition*, John Wiley & Sons, Inc. New York.

Fjar, E., R.M. Holt, P. Horsrud, and A.M. Raaen, 1991. *Petroleum Related Rock Mechanics*. Elsevier, Amsterdam.

Harris, 2006. Seismic Monitoring of CO2 Sequestration, GCEP Technical Report. Stanford University.

Hart, D.J., 2000. Laboratory Measurements of Poroelastic Constants and Flow Parameters and Some Associated Phenomena, Ph.D. Thesis, University of Wisconsin–Madison.

Hart, D.J., K.R. Bradbury, and D.T. Feinstein, 2006. The vertical hydraulic conductivity of an aquitard at two spatial scales, *Ground Water*, 44(2), 201–211.

Muggeridge, A., Y. Abacioglu, W. England, and C. Smalley, 2004. Dissipation of anomalous pressures in the subsurface, *Journal of Geophysical Research*, 109, B11104, doi:10.1029/2003JB002922.

Neuzil, C.E., 1994. How permeable are clays and shales? *Water Resources Research*, 30(2), 145–150.

Neuzil, C.E., 1995. Abnormal pressures as hydrodynamic phenomena, *American Journal of Science*, 295, 742-786.

Pruess, K, 2005. ECO2N: A TOUGH2 Fluid Property Module for Mixtures of Water, NaCl, and CO_2, LBNL-57952, Lawrence Berkeley National Laboratory, Berkeley, California.